Inorganic Chemistry

Article

pubs.acs.org/IC

Computational Examination of the Mechanism of Alkene Epoxidation Catalyzed by Gallium(III) Complexes with N-Donor Ligands

Michael L. McKee* and Christian R. Goldsmith*

Department of Chemistry and Biochemistry, Auburn University, Auburn, Alabama 36849, United States

Supporting Information

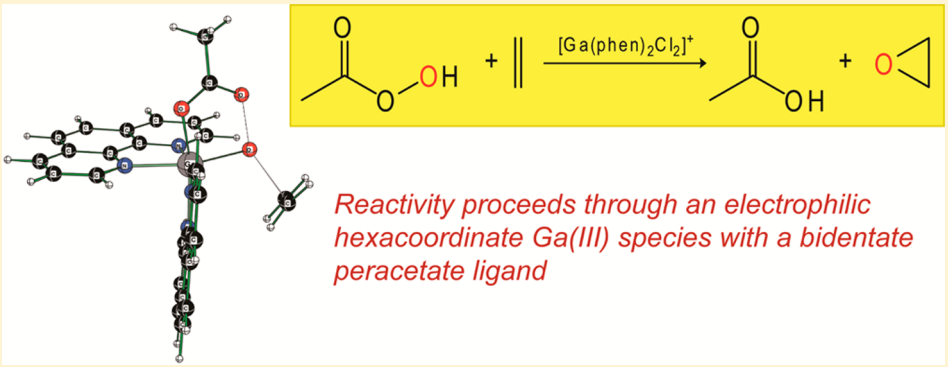

ABSTRACT: The ability of gallium(III) complexes to catalyze the epoxidation of alkenes by peracetic acid has been examined with density functional theory calculations. According to the calculations, the chloride anions of the precatalyst $[Ga(phen)_2Cl_2]^+$ (phen = 1,10-phenanthroline) can be displaced by either acetic or peracetic acid through dissociative ligand exchange pathways; both acetic and peracetic acid deprotonate upon binding to the formally tricationic metal center. Because of the high basicity of peracetate relative to that of chloride, only the acetate for chloride exchange occurs spontaneously, providing a rationale for the preponderance of gallium acetate adducts observed in the reaction mixtures. With respect to the mechanism of olefin epoxidation, the computational results suggest that the peracetic acid is most efficiently activated for redox activity when it binds to the metal center in a κ^2 fashion, with the carbonyl oxygen atom serving as the second point of attachment. The phen ligands' coordination to the gallium is essential for the catalysis, and the lowest energy pathways for alkene oxidation proceed through hexacoordinate Ga(III) species with four Ga−N bonds. A natural bond order analysis confirms the electrophilic nature of the metal-containing oxidant.

INTRODUCTION

Gallium(III) compounds have been found to serve as homogeneous catalysts for a wide range of chemical transformations.[1−7] Although most of these catalyzed reactions involve acid/base reactivity, Ga(III) complexes have also been found to promote oxidation−reduction reactions in rare instances.[8−12] Recently, one of our laboratories reported that $[Ga(phen)_2Cl_2]Cl$ (phen = 1,10-phenanthroline)[13−15] and related Ga(III) complexes with N_4Cl_2 coordination spheres can catalyze the epoxidation of alkenes by peracetic acid (PA).[16,17] When the ratio of PA to Ga(III) is sufficiently low (200:1 or less), the catalyzed oxidation yields epoxides as the sole organic products. Both the selectivity for the epoxide and the rate of reaction at ambient temperatures are superior to those of other systems for alkene epoxidation that use a group 13 element in a catalytic capacity.[18−20]

The mechanisms of these reactions are difficult to probe experimentally. The diamagnetism of Ga(III), in particular, severely limits the spectroscopic interrogation of catalytically relevant species. A peracetate complex with Ga(III) is believed to be responsible for the oxygen atom transfer, but such adducts have not yet been observed.[16,17] Mass spectrometry instead detects exclusively Ga(III) acetate adducts during the reactions, with the acetates substituting for the chlorides initially bound to the metal ion. Removal of the acetic acid component of the added PA is not feasible, due to the extreme hazards posed by highly concentrated solutions of peracids.[21] The high concentrations of acetic acid and, to a lesser extent, PA relative to the gallium preclude identification and characterization of mechanistically relevant adducts by nuclear magnetic resonance.

Some mechanistic insight has been obtained by analyzing how changes in the alkene substrate and N-donor ligand impact the epoxidation activity. The oxygen transfer agent is likely electrophilic, given that the more electron-rich substrates *cis*-cyclooctene and cyclohexene react at faster rates and to greater extents than the relatively electron-deficient terminal alkenes 1-

Received: September 4, 2013
Published: December 5, 2013

octene and styrene.[16,17] The activities of Ga(III) complexes with electronically modified phen ligands also support the agency of an electrophilic oxidant. Installing nitro groups at the 5-positions of the phen ligands increases the turnover frequency; conversely, the addition of electron-donating amino groups at the 5-positions decreases the epoxidation activity.[17] The Ga(III) is catalytically inactive in the absence of the N-donor ligands,[16] and substituting a tetradentate ligand in place of two bidentate ligands prolongs the catalysis, consistent with the necessity of a stable $[GaN_4]^{3+}$ core for reactivity.[17] Additional ligand donor atoms, however, decrease the activity, as evidenced by the lower yields of epoxides associated with the potentially pentadentate *N,N,N′*-tris(2-pyridylmethyl)-1,2-ethanediamine (trispicen) and the potentially hexadentate *N,N,N′,N′*-tetrakis(2-pyridylmethyl)-1,2-ethanediamine (tpen).[17] The additional ligating groups may compete with the terminal oxidant for coordination sites on the Ga(III). Given that inhibition is observed with a fifth donor atom, this may suggest that the PA is bidentate, as opposed to monodentate, in the oxygen atom transferring species (Scheme 1). Alternatively,

Scheme 1. Most Plausible Modes of PA Coordination in Oxygen-Transferring Species

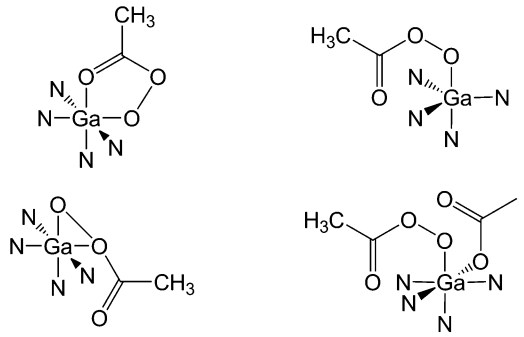

κ-2 modes of coordination κ-1 modes of coordination

the additional arms may impede reactivity by blocking PA coordination and/or substrate access to the reactive portion of the oxygen-transferring species through steric effects. The observed hypodenticities of the trispicen and tpen ligands to the Ga(III) in acetonitrile solution[17] may be more consistent with the second possibility.

In an effort to better understand the mechanism of gallium-catalyzed epoxidation, we have probed the gallium speciation chemistry and the structures of the most plausible oxidants with density functional theory (DFT) calculations. Similar analyses have been performed for other catalysts for alkene epoxidation,[22−26] including $[Al(H_2O)_6]^{3+}$.[20] Specifically, we investigate the free energy pathways corresponding to κ^1 and κ^2 coordination of the PA. The computations focus on the reactivity of the complex $[Ga(phen)_2Cl_2]^+$ (**1Cl$_2$**; Scheme 2), which has the benefit of being structurally characterized.[16]

EXPERIMENTAL SECTION

Computational Methodology. The Gaussian 09 program was used for all calculations.[27] All geometries were optimized at the B3LYP/6-31G(d) level, with the starting geometry of the $[Ga(phen)_2Cl_2]^+$ cation coming from a previous study.[16] Vibrational frequencies were computed at that level to confirm the nature of the stationary point and to make zero-point, temperature, and entropy corrections to 298 K. Solvation free energies in acetonitrile (MeCN) were computed at the SMD/B3LYP/6-31+G(2d,p) level. The solution

Scheme 2. Structure of $[Ga(phen)_2Cl_2]^+$ (1Cl$_2$)

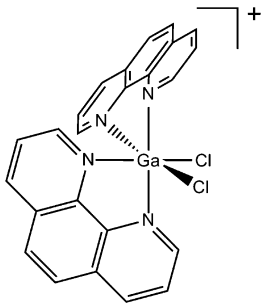

free energies were determined from ΔG(an,298 K) = ΔG(g,298 K) + ΔG(solv,298 K).

The transition vectors of all transition states were animated to confirm that the motion would convert the reactant into the product. If the motion was not clear, the transition state structure was distorted in both directions (reactant and product) and reoptimized to confirm the identity of the corresponding minima.

The epoxidation reaction proceeding through the intermediate predicted from the B3LYP/6-31G(d) results was also investigated with the more rigorous M05-2X/6-311+G(2d,p) DFT methodology.[28] In these calculations, M05-2X/6-311+G(2d,p) provided the zero-point correction, thermal correction, and $T\Delta S$ terms; the ΔG(solv,298 K) term was calculated from SMD/B3LYP/6-31+G(2d,p).

RESULTS

Speciation of Ga(III) in the Reaction Mixture. The previously described epoxidation reaction solutions consist of a mixture of $[Ga(phen)_2Cl_2]Cl$, acetonitrile (MeCN), acetic acid (AC), and peracetic acid (PA).[16] An understanding of the gallium speciation chemistry is essential to determining the most favorable pathways for olefin epoxidation. Given the basicity of chloride in MeCN (pK_a of HCl 10.3),[29] AC or PA for chloride ligand exchange is anticipated to produce a gallium peracetate adduct and HCl, rather than a gallium peracetic acid complex and free Cl^-. The stabilities of $[Ga(phen)_2]^{3+}$ cores (**1**) with various exogenous ligand sets containing MeCN, chloride, acetate (AI), and peracetate (PI) were consequently assessed with DFT calculations. Gas-phase values were calculated and then corrected for the MeCN medium.

As shown in Figure 1, complexes with two anionic O-donor ligands in the inner sphere tend to be the most stable. Direct comparisons of differently charged species are complicated by uncertainties in their relative free energies of solvation; consequently, the values in Figure 1 should be viewed as approximations. MeCN, being a neutral ligand with a much higher pK_a than either AC or PA, cannot displace the chlorides to a significant degree, since it would result in a tricationic species. This finding is consistent with previously reported experimental results; in the absence of AC and PA, the $[Ga(phen)_2Cl_2]^+$ complex (**1Cl$_2$**) and related species are indefinitely stable in dry MeCN.[16,17] The O-donor ligands are found to bind more strongly to the Ga(III) than the chloride, to the extent that the complexes with a single AI or PI ligand have lower free energies than either **1Cl$_2$** or the $[Ga(phen)_2(Cl)(AI)]^+$ species (**1ClAI**). The ability of AI and PI to bind in a bidentate fashion is essential for the stabilization of the dicationic $[Ga(phen)_2(\kappa^2\text{-AI})]^{2+}$ (**1AI**) and $[Ga(phen)_2(\kappa^2\text{-PI})]^{2+}$ (**1PI**) over the monocationic $[Ga(phen)_2(Cl)(AI)]^+$ (**1ClAI**). Pentacoordinate analogues of these first two species with monodentate AI and PI ligands are less stable by 8.2 and 7.3 kcal mol^{-1}, respectively. The

dx.doi.org/10.1021/ic402261v | Inorg. Chem. 2014, 53, 318−326

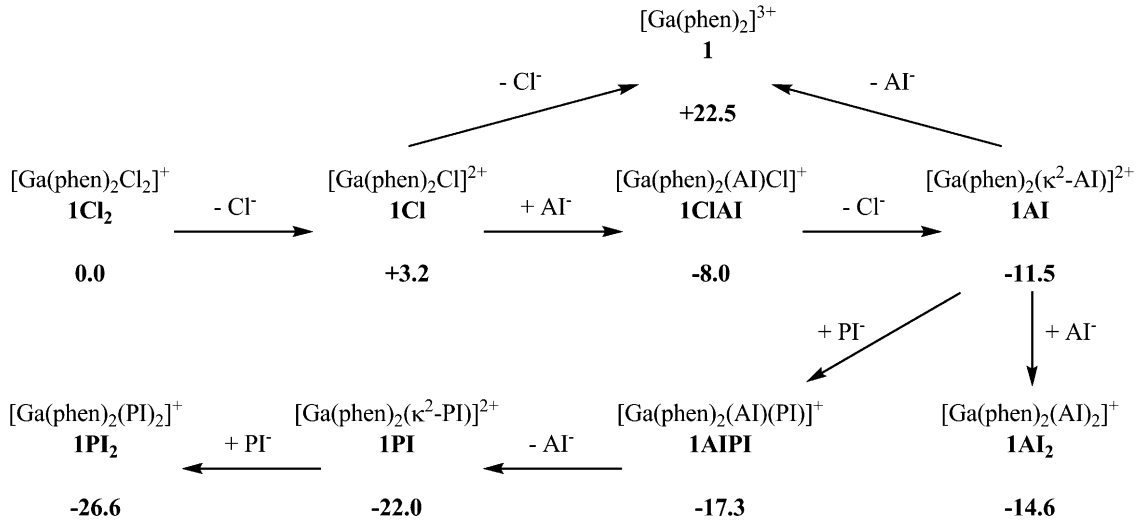

Figure 1. ΔG(MeCN, 298 K) of selected $[Ga(phen)_2]^{3+}$ (**1**) containing species calculated from the SMD/B3LYP/6-31+G(2d,p)//B3LYP/6-31G(d) method. All free energies are reported in kcal mol^{-1} relative to $[Ga(phen)_2Cl_2]^+$ (**1Cl$_2$**).

experimental results indicate that the phen ligands eventually dissociate from the Ga(III), presumably forming $[Ga(OAc)_3]$. Our calculations suggest that this process is spontaneous for substitution by AI (eq 1) and weakly spontaneous, at best, for

$$[Ga(phen)_2(OAc)]^{2+} + 2AcO^- \rightarrow [Ga(OAc)_3] + 2phen \quad \Delta G(an, 298\ K) = -17.5\ kcal\ mol^{-1} \quad (1)$$

$$[Ga(phen)_2(OAc)]^{2+} + 2AcOH \rightarrow [Ga(OAc)_3] + 2phenH^+ \quad \Delta G(an, 298\ K) = 4.2\ kcal\ mol^{-1} \quad (2)$$

displacement by AC (eq 2, with an approximate error of ±5 kcal mol^{-1} for ΔG(an,298 K)).[30] Although eventual loss of the phen is highly likely, the full detachment of a phen ligand has not been observed in any optimized structures.

The chlorides can be displaced by PA or AC through a number of different mechanisms. The acid present may facilitate these exchanges by protonating the leaving group Cl^- to allow the loss of a neutral, rather than a charged, species into the MeCN solvent. Calculations were performed to determine whether the Cl^- leaves the gallium's coordination sphere before or after the ligation of the entering group. The lowest energy pathways for ligand exchange featuring the loss of the Cl^- after the association of the entering group appear to proceed through six-coordinate species in which one of the phen ligands is partially detached from the metal; the Cl^- dissociates in the form of HCl upon reattachment of the N donor to the Ga(III) (Figure 2). The lack of heptacoordinate intermediates suggests that each elementary step proceeds through an interchange mechanism. Even though these species are stabilized by hydrogen-bond interactions between the AC and the leaving group chloride, the free energy barriers are higher than that for a dissociative pathway that proceeds through a five-coordinate Ga(III) intermediate (Figure 3). Substitution by PI is likewise predicted to occur through a dissociative pathway with transient pentacoordinate Ga(III) intermediates. The free energies for the ligand exchange reactions in Figures 2 and 3 differ from those shown in Figure 1, since the former account for the acids and anions consumed and produced by the ligand substitutions. Some of the transition states have lower free energies than adjoining intermediates once zero-point, thermal, and entropy corrections are made; this may suggest that these intermediates are bypassed during the reaction pathway.

The transition states for the elimination and addition of chloride, acetate, and peracetate are not shown in Figure 1. Each anion elimination reaction increases the charge of the gallium complex from 1+ to 2+. In the gas phase, these eliminations are endothermic by almost 100 kcal mol^{-1}. Because of its relevance, the dissociation of **1Cl$_2$** to **1Cl** and Cl^- was investigated in more detail (Figure 4). To compute the reaction coordinate, the distance between the Ga(III) and the departing Cl^- was fixed and optimized, with adjustments for solvation effects, by SMD/B3LYP/6-31G(d). The transition vector was projected out of the Hessian for points along the reaction coordinate when making zero-point, thermal, and entropy corrections. Solvation energies were computed at the SMD/B3LYP/6-31+G(2d,p)//SMD/B3LYP/6-31G(d) level. The free energy profile shows a maximum at 3.5 Å with a free energy barrier of 9.2 kcal mol^{-1} in MeCN at 298 K. The plot of the reaction coordinate (Figure 4) shows the electronic energy exceeding 70 kcal mol^{-1} as the Ga−Cl distance increases to 10 Å. Elimination barriers were not computed for AI and PI, but these free energy barriers should be similar to that of the chloride reaction, given that the charges of the relevant ions are identical.

Mechanism of Alkene Epoxidation. The mechanism of alkene epoxidation was investigated using ethylene as a substrate. Although the Ga(III) complexes have not been observed to catalyze the oxidation of this molecule by PA, ethylene represents a minimally sized model substrate for the calculations.

Two major classes of pathways were investigated, with a focus on identifying the gallium-containing oxygen transfer agent. The first entailed oxygen atom transfer from complexes with one or more κ^1 PI ligands, such as $[Ga(phen)_2(AI)(PI)]^+$ (**1AIPI**, Figure 5). The second explored the κ^2 species **1PI** as the active oxidant (Figure 6). The results suggest that **1PI** is the superior oxidant; its free energy of activation of 33.3 kcal mol^{-1} (TS8) is almost 7 kcal mol^{-1} less than that for **1AIPI** (TS7)

dx.doi.org/10.1021/ic402261v | Inorg. Chem. 2014, 53, 318−326

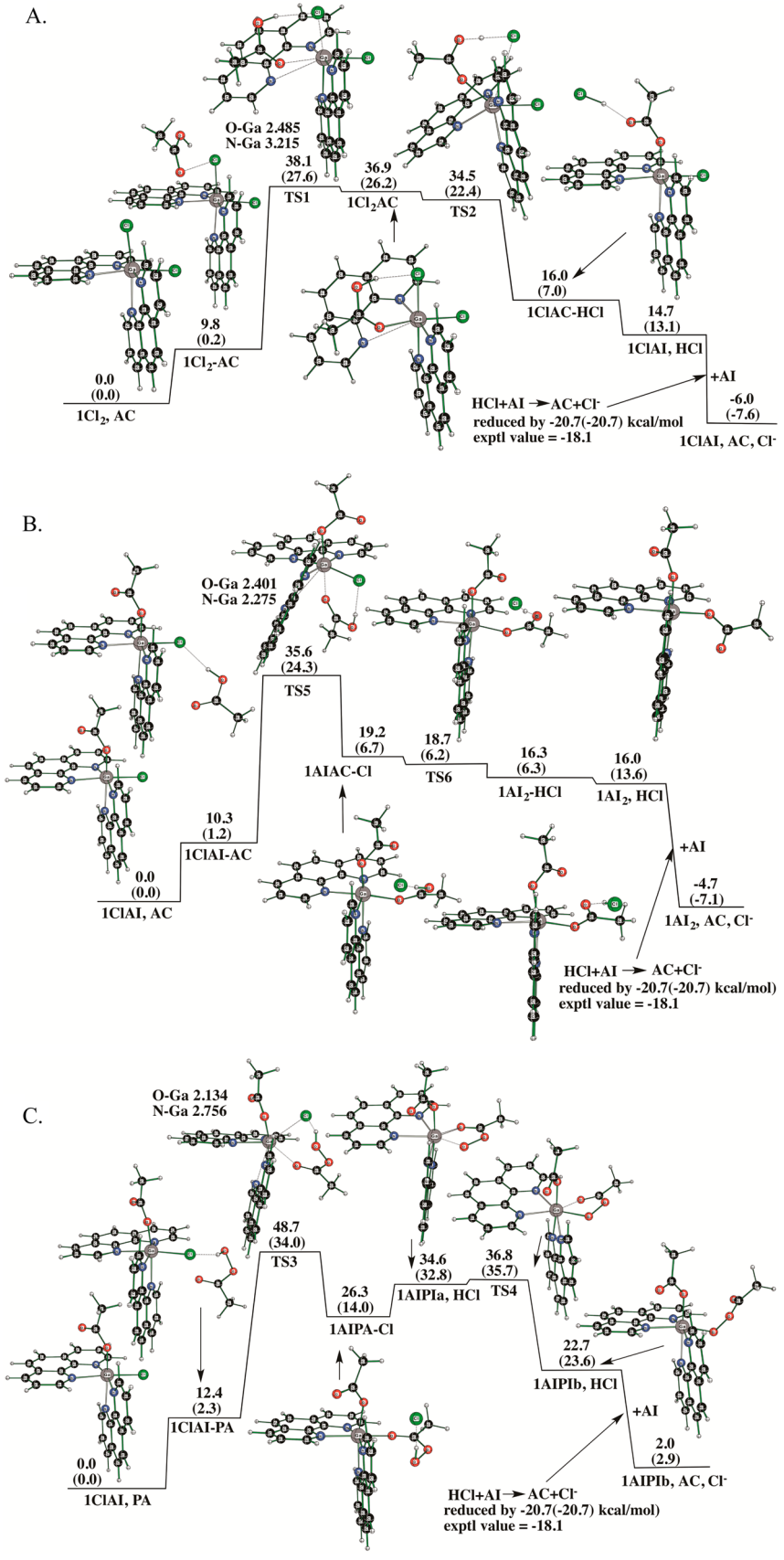

Figure 2. Free energy analysis of ligand exchange pathways for the $[Ga(phen)_2]^{3+}$ core: (A) substitution of acetate for chloride on $[Ga(phen)_2Cl_2]^+$ (**1Cl$_2$**) to yield $[Ga(phen)_2(AI)(Cl)]^+$ (**1ClAI**); (B) substitution of acetate for chloride on **1ClAI** to yield $[Ga(phen)_2(AI)_2]^+$ (**1AI$_2$**); (C) substitution of peracetate for acetate on **1ClAI** to yield $[Ga(phen)_2(AI)(PI)]^+$ (**1AIPI**). In each displayed pathway, the Cl^- is lost after the initial ligation of the entering group. All relative energies are in kcal mol^{-1}. The values in parentheses are enthalpies in 298 K MeCN.

dx.doi.org/10.1021/ic402261v | *Inorg. Chem.* 2014, 53, 318−326

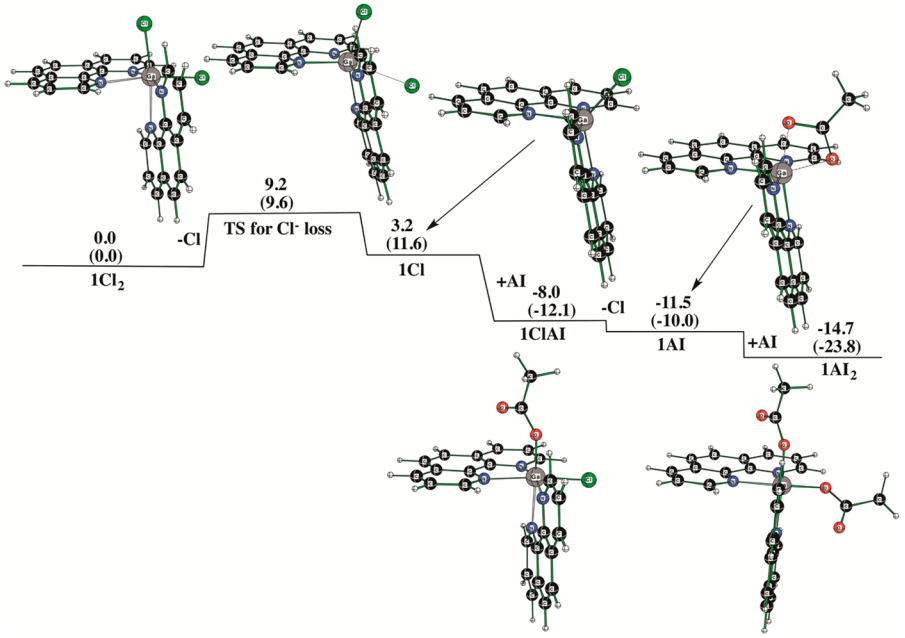

Figure 3. Free energy analysis of the dissociative exchange pathways for acetate substitution for chloride on $\mathbf{1Cl_2}$ and **1ClAI** to yield **1ClAI** and $\mathbf{1AI_2}$, respectively. All energies are reported in kcal mol^{-1} relative to $\mathbf{1Cl_2}$. The values in parentheses are enthalpies in 298 K MeCN.

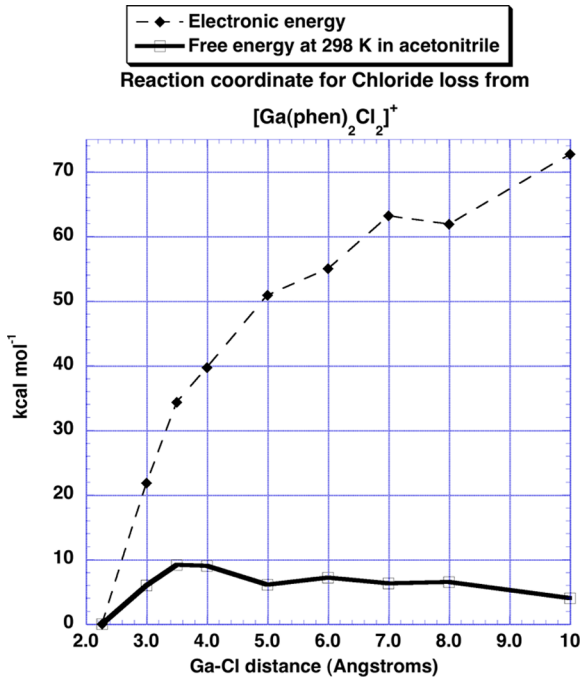

Figure 4. Analysis of the electronic energy and 298 K free energy of $\mathbf{1Cl_2}$ as one of the Ga−Cl bonds is systematically elongated. The calculations predict a free energy barrier of 9.2 kcal mol^{-1} for the dissociation of the complex to **1Cl** and Cl^-.

after the approaches of the ethylene are optimized. The barrier has a stronger enthalpic component at 298 K, with $\Delta H^{\ddagger}$ = 22.9 kcal mol^{-1}. In all considered mechanisms, the loss of the ethylene oxide (EO) product from a common **1AIEO** intermediate is facilitated by the presence of a bound acetate, which shifts from monodentate to bidentate coordination upon loss of EO. In the transition state corresponding to the oxygen atom transfer, the O−C bonds between the transferred oxygen atom and the ethylene's carbon atoms are 2.168 and 2.199 Å (Figure 7). The near-equivalence of these bonds suggests that the O atom transfer occurs through a concerted process, rather than a sequence of one-electron steps. The Ga−N bond lengths in the transition state average 2.094 Å, nearly identical to the 2.108 Å average for the structurally characterized $[Ga(phen)_2Cl_2]^+$.[16] The pathway proceeding through **1PI** was also investigated with more rigorous M05-2X/6-311+G(2d,p) DFT calculations. In these calculations, M05-2X/6-311+G(2d,p) provided the zero-point correction, thermal correction, and $T\Delta S$ terms; the ΔG(solv,298 K) term, conversely, came from SMD/B3LYP6-31+G(2d,p). These predict a similar free energy barrier for ethylene epoxidation of 37.8 kcal mol^{-1} and an earlier transition state, as indicated by the longer C−O bonds (2.090 and 2.149 Å).

The reactivity was also assessed with cyclohexene as the oxygen atom acceptor (Figure 8). This alkene does serve as a competent substrate for gallium-catalyzed epoxidation and is oxidized to cyclohexene oxide.[16,17] As anticipated, the use of this more electron-rich alkene lowers the free energy barrier for epoxidation. However, the $\Delta G^{\ddagger}$ value is higher than would be expected for a reaction that occurs readily at 298 K.[16] This may suggest that the calculated entropic contribution is too high. The reaction pathway remains fundamentally unchanged from that calculated for the ethylene oxidation and proceeds through the same **1PI** intermediate.

A natural bond orbital (NBO)[31,32] and natural energy decomposition analysis (NEDA)[33] using NBO-5.9[34] shows that the dominant interaction in the transition state is electron donation from the occupied π orbital of the olefin into the elongated σ^* O−O orbital of the ligated peracetate (Figure 9, Table 1). In contrast, the electron donation from the lone pair of the transferred oxygen into the unoccupied π^* of the olefin is 5.0 and 5.6 times smaller in TS8 and TS9, respectively. For the epoxidation of ethylene, two orientations of the substrate were calculated (TS8 and TS88). In TS88 the ethylene is rotated by 90°, such that its C═C bond is no longer parallel to the proximal phen ring system. The free energy barrier for TS88 is

dx.doi.org/10.1021/ic402261v | Inorg. Chem. 2014, 53, 318−326

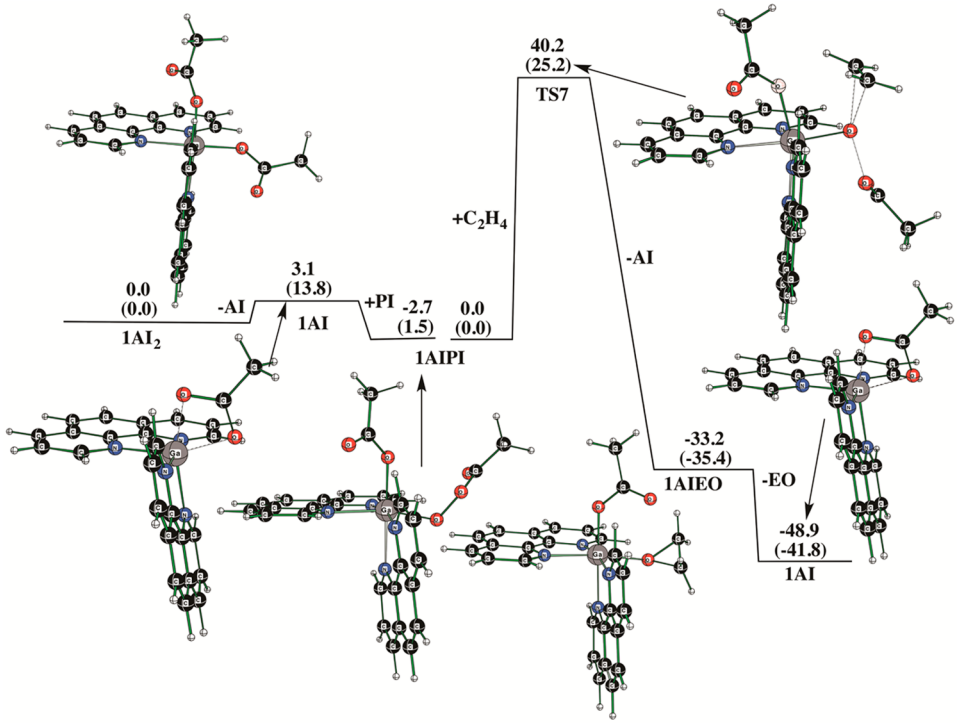

Figure 5. Free energy analysis of ethylene epoxidation by $[Ga(phen)_2(AI)(PI)]^+$ (**1AIPI**) to yield **1AI** and ethylene oxide (EO). EO is transiently bound to the Ga(III) (**1AIEO**). All energies are reported in kcal mol^{-1} relative to $\mathbf{1AI_2}$. The values in parentheses are enthalpies in 298 K MeCN.

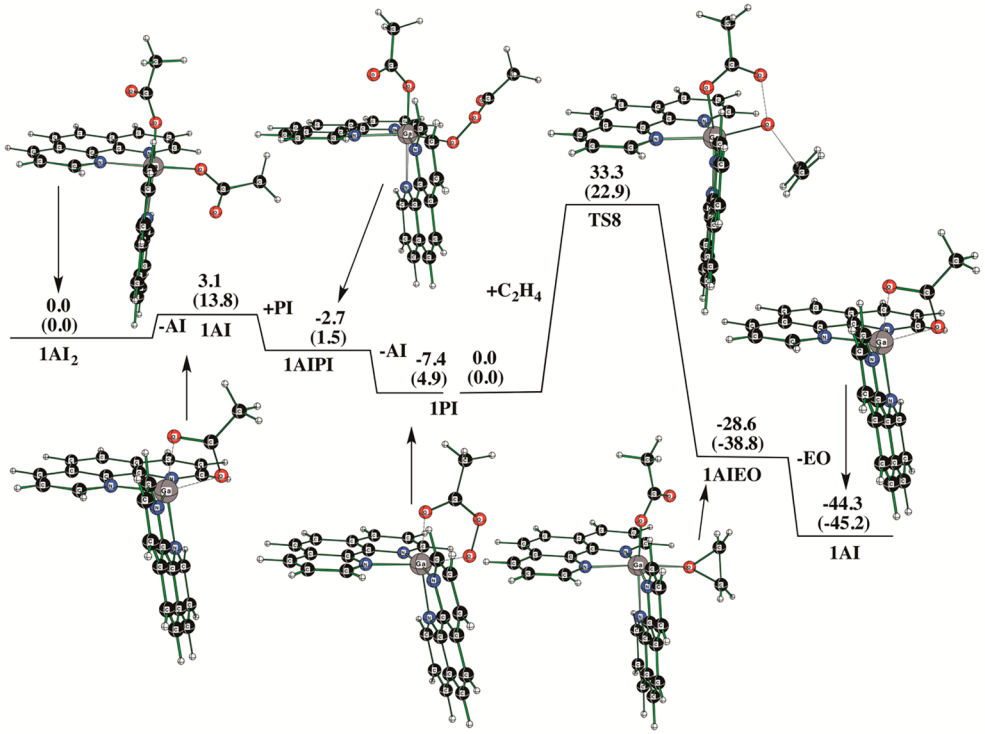

Figure 6. Free energy analysis of ethylene epoxidation by $[Ga(phen)_2(PI)]^{2+}$ (**1PI**) to yield **1AI** and **EO**. Note that the PI is bound in a bidentate fashion. EO is transiently bound to the Ga(III) in the **1AIEO** complex. All energies are reported in kcal mol^{-1} relative to $\mathbf{1AI_2}$. Enthalpies calculated for the species in 298 K MeCN are given in parentheses.

higher by 1.3 kcal mol^{-1} than that of TS8. Although the two transition states have similar free energies for ethylene, the differences will likely be greater for bulkier substrates. Although the interactions between the Ga(III) species and the olefin are attractive overall, the barrier is positive, since both fragments must distort from their optimum structures in order to reach the transition state geometry. It is noteworthy that the total interaction between the two fragments is much larger for the epoxidation of ethylene (TS8, 80.1 kcal mol^{-1}) in comparison to cyclohexene (TS9, 56.1 kcal mol^{-1}). Given that the double

dx.doi.org/10.1021/ic402261v | *Inorg. Chem.* 2014, 53, 318−326

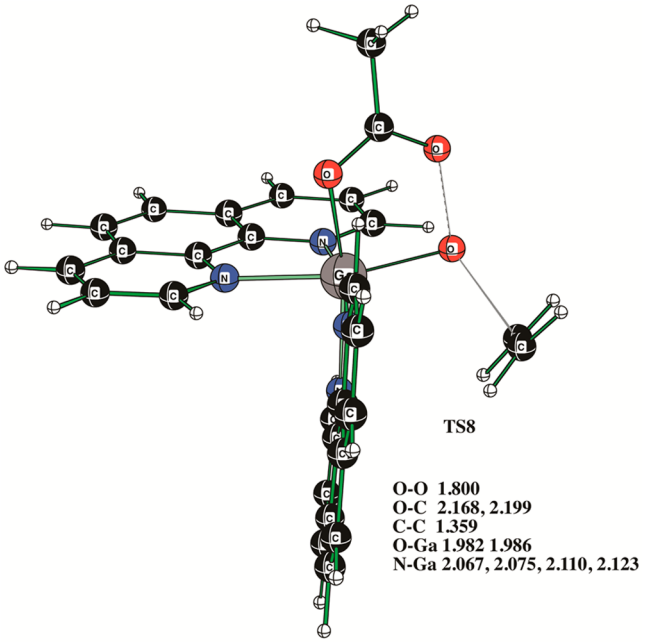

Figure 7. Calculated structure of the transition state TS8 from Figure 6

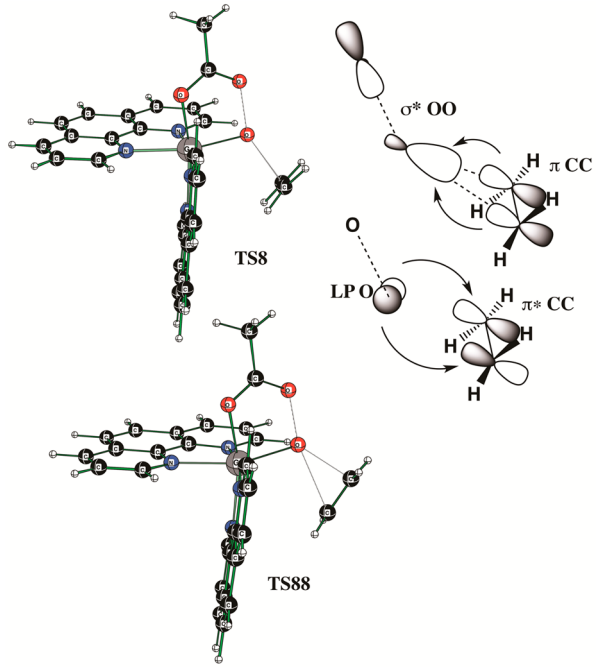

Figure 9. NBO analysis of the interactions between the **1PI** oxidant and ethylene in the two lowest energy transition states.

bond in cyclohexene is more electron-rich than that in ethylene, this is a counterintuitive result. Comparison of the two reactions is likely obfuscated by the differing time points of the transition states. Presumably, the fragments in TS8 must distort more than those in TS9 to attain the transition state geometry. However, the ratio of the olefin→Ga to Ga→olefin interactions, which should be independent of the time point of the transition state, is larger for TS9 (5.6) than for TS8 (5.0), as would be expected for the more electron rich double bond of cyclohexene.

DISCUSSION

The approximate stabilities of the $[Ga(phen)_2(AI)_2]^+$ (**1AI$_2$**), $[Ga(phen)_2(AI)(PI)]^+$ (**1AIPI**), and $[Ga(phen)_2(PI)_2]^+$ (**1PI$_2$**) species relative to those of the chloride complexes described in Figure 1 can be rationalized by considering the hardness of the relevant bases and acids and the increased stability associated with charge neutralization. The Ga(III) ion is widely perceived to be a hard acid and commonly forms strong bonds with hard bases, such as anionic O donors.[35] Chloride is empirically observed to be a softer base than most O-donor ligands;[36] consequently, **1Cl$_2$** is less stable than the analogously charged **1AI$_2$**, **1AIPI**, and **1PI$_2$**. The presence of two anionic ligands in the inner sphere should lower the free energy of the complex through Coulombic effects. The products of MeCN for chloride exchange, conversely, lead to increased charge separation in the products; consequently, these displacements

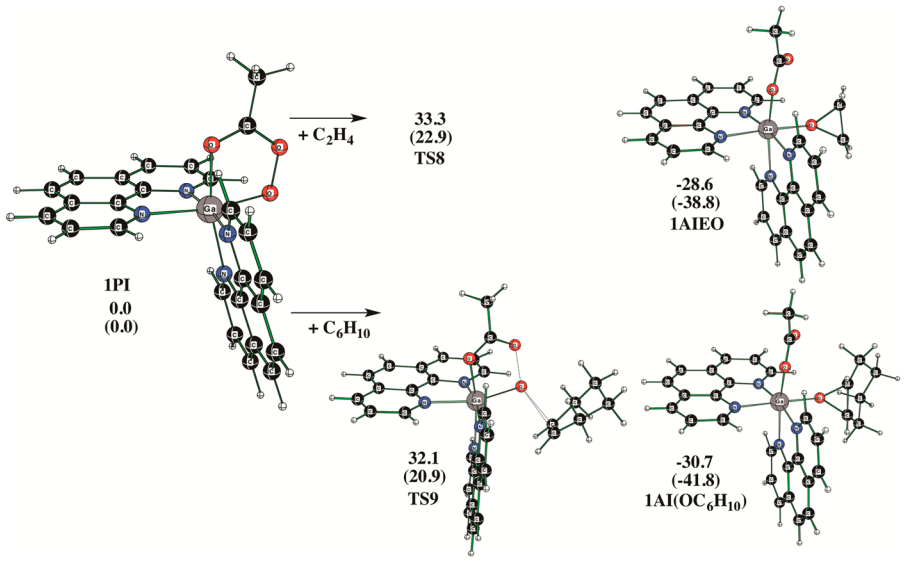

Figure 8. Comparison of the transition state free energies (kcal mol^{-1}) for the oxidation of ethylene and cyclohexene by **1PI**. All energies are relative to that of **1PI**. Enthalpies for the species in 298 K MeCN are given in parentheses.

dx.doi.org/10.1021/ic402261v | *Inorg. Chem.* 2014, 53, 318−326

Table 1. NBO and NEDA of the Interactions (kcal mol^{-1}) between the Olefin and 1PI Oxidant in the Transition State Geometries at the B3LYP/6-31G(2d,p) Level

	olefin ($\pi_{C=C}$)→ **1PI** (σ^*_{O-O})[a]	**1PI** (LP_O)→ olefin ($\pi^*_{C=C}$)[a]	sum	total interaction[b]	total, %[c]	ratio[d]
		Olefin = Ethylene				
TS8	58.0	11.7	69.7	80.1	87	5.0
TS88	55.1	11.7	69.8	89.3	78	3.7
		Olefin = Cyclohexene				
TS9	33.6	6.0	39.6	56.1	70	5.6

[a]Calculated from NBO second-order perturbation theory analysis of transition states for olefin epoxidation by **1PI**. [b]From NEDA. [c]Percent contribution of $\pi_{C=C}\rightarrow\sigma^*_{O-O}$ and $LP_O\rightarrow\pi^*_{C=C}$ interactions to the total interaction between the olefin and GaPI in the given transition state. [d]Ratio of olefin ($\pi_{C=C}$)→**1PI** (σ^*_{O-O}) to **1PI** (LP_O)→olefin ($\pi^*_{C=C}$) interaction energies.

are highly unfavorable from a free energy perspective and are not observed experimentally.[16,17]

The calculations predict that $[Ga(phen)_2]^{3+}$ cores with a single, bidentate, anionic ligand are particularly stable; the added stability can be attributed to chelate effects. The κ^2 coordination of the peracetate anion results in a five-membered metallacycle which has much lower ring strain than the four-membered metallacycle that results from acetate coordination.[37] **1PI** is therefore intrinsically more stable than **1AI** (Figure 1). Mass spectrometry of the Ga(III) species formed from the reaction between $[Ga(phen)_2Cl_2]Cl$ and a large excess of PA (added as a 7.1% molar solution in AC) reveals m/z features consistent with $[Ga(phen)_2(AI)]^{2+}$ (**1AI**). This species could also result from loss of an anion from either $\mathbf{1AI_2}$ or **1AIPI**.[16] Although the Ga(III) complexes with PI are intrinsically more stable, the greater basicity of PI relative to Cl^- makes these reactions energetically unfavorable when the fate of the leaving group is considered (Figure 2) and explains why **1PI** and **1AIPI** complexes have not yet been observed experimentally. The difference in basicity between AI and Cl^- is smaller, and the stabilities of **1ClAI** and $\mathbf{1AI_2}$ relative to $\mathbf{1Cl_2}$ and **1ClAI** are sufficient to render acetate for chloride exchange thermodynamically favorable under catalytic conditions.

The ligand exchange is predicted to occur through a dissociative mechanism, in which the loss of the Cl^- precedes the introduction of either AI or PI into the gallium's coordination sphere (Figure 3). The results are reminiscent of those recently reported by Novikov et al., who calculated that the substitution of water by hydrogen peroxide in $[Ga(H_2O)_6]^{3+}$ also proceeds through a dissociative mechanism.[38]

The oxygen transfer agent is predicted to be $[Ga(phen)_2(PI)]^+$ (**1PI**), with the peracetate binding in a bidentate fashion through the terminal O atom in the O−O bond and the O atom from the carbonyl (Figures 6 and 7). The coordination of the peracetate resembles that previously observed and calculated for iron and nickel complexes with PI.[39−41] The structure of **1PI** differs from those of the oxygen transfer agents predicted from mixtures of $[Al(H_2O)_6]^{3+}$ and H_2O_2 in that the latter have both O atoms from the O−O bond of the terminal oxidant bound to the metal, resulting in a three-membered ring.[20] The lesser ring strain associated with the five-membered metallacycle in the Ga^{III}/PA system would favor this linkage isomer over the three-membered ring resulting from the coordination of both peroxyl O atoms (Scheme 1).[37] Previously, we found that gallium-catalyzed alkene epoxidation in MeCN failed when H_2O_2 was used as a terminal oxidant.[16,17] Bidentate coordination of this molecule would necessarily proceed through a far less stable three-membered metallacycle; the relative instability of this intermediate may preclude gallium-catalyzed alkene epoxidation by H_2O_2. A recent theoretical examination of $HO^\bullet$ radical generation from H_2O_2 and group 13 metal aqua complexes found that H_2O_2 tended to bind to Ga(III) in a κ^1, rather than a κ^2, mode.[38] From these considerations, we would expect the epoxidation chemistry of the Al(III) system to improve upon substituting PA for H_2O_2, since this would allow access to less ring strained oxidants. Although the activity would be anticipated to be higher with PA, H_2O_2 is a more attractive terminal oxidant from both economic and environmental vantages.

The need for bidentate coordination of the PI is consistent with the less extensive catalysis associated with $[Ga(tpen)Cl_2]^+$ and $[Ga(trispicen)Cl_2]^+$, which have one or two pendent pyridine rings capable of competing for coordination sites on the metal ion.[17] Another factor that may contribute to the inadequacy of H_2O_2 as a terminal oxidant is that the O−O bond cleaves to generate a hydroxide leaving group, which is less stable than the acetate leaving group that results from the reduction of PA. One might expect this effect to be mitigated by switching to a more polar solvent with a higher tolerance for charged species, but H_2O_2 was found to be ineffective as a terminal oxidant in gallium-catalyzed alkene epoxidation reactions run in water.

Another key difference between the aluminum and gallium alkene epoxidation systems is that the oxygen atom transferring agents in the gallium chemistry are predicted to be exclusively hexacoordinate, whereas the active oxidants in the aluminum chemistry were calculated to be a mixture of penta- and hexacoordinate Al(III) complexes.[20] This is readily rationalized by the greater ionic radius of Ga(III) relative to Al(III), which would support higher coordination numbers, and the strong coordination by the two phen ligands to the metal ion during the catalysis. Although one Ga^{III}−N bond was observed to temporarily break during potential pathways for ligand exchange (Figure 2), this was not observed in the lowest energy pathways for alkene epoxidation.

NBO and NEDA studies of the transition state suggest that the primary interaction between the **1PI** species and the alkene substrate involves electron transfer from the π bond of the alkene to the σ^* bond between the two O atoms in the bound peracetate (Figure 9, Table 1). This suggests that the reactivity can be facilitated by enhancing either the nucleophilicity of the substrate or the electrophilicity of the **1PI** complex. A comparison of the oxidations of ethylene and cyclohexene is complicated by the earlier transition state predicted for cyclohexene. The calculated ratios of the interactions, however, are consistent with previously obtained experimental results, which demonstrated that more electron rich C=C groups react more readily and that Ga(III) complexes with more poorly electron-donating ligands tend to exhibit faster catalysis.[16,17]

CONCLUSIONS

The oxygen-transferring agent in the gallium-catalyzed epoxidation of alkenes by peracetic acid is predicted by DFT calculations to be $[Ga(phen)_2(PI)]^{2+}$. The PI displaces acetate ions from the Ga(III) center and coordinates the metal center in a bidentate fashion, forming a relatively stable five-membered

dx.doi.org/10.1021/ic402261v | Inorg. Chem. 2014, 53, 318−326

metallacycle. Analysis of the transition state indicates that the peracetate oxidant is highly electrophilic, in agreement with previously obtained experimental results.

■ ASSOCIATED CONTENT

Supporting Information

Table S1, giving charge, point group, absolute energies, zero-point energy and thermal corrections, entropies, and free energies of solvation in MeCN for all relevant species, and Table S2, giving Cartesian coordinates for all calculated intermediates and transition states optimized at the B3LYP/6-31G(d) level. This material is available free of charge via the Internet at http://pubs.acs.org.

■ AUTHOR INFORMATION

Corresponding Author

*E-mail: mckeeml@auburn.edu (M.L.M.), crgoldsmith@auburn.edu (C.R.G.).

Notes

The authors declare no competing financial interest.

■ ACKNOWLEDGMENTS

The authors are grateful for funding provided by Auburn University. Ms. Sharon Ting attempted the aqueous olefin epoxidation reactions mentioned in the Discussion. Computer time was provided by the Alabama Supercomputer Network.

■ REFERENCES

(1) Dagorne, S.; Atwood, D. A. *Chem. Rev.* **2008**, *108*, 4037−4071.
(2) Yamaguchi, M.; Nishimura, Y. *Chem. Commun.* **2008**, 35−48.
(3) Wehmschulte, R. J.; Steele, J. M.; Young, J. D.; Khan, M. A. *J. Am. Chem. Soc.* **2003**, *125*, 1470−1471.
(4) Cowley, A. H. *J. Organomet. Chem.* **2000**, *600*, 168−173.
(5) Lichtenberg, C.; Spaniol, T. P.; Okuda, J. *Inorg. Chem.* **2012**, *51*, 2254−2262.
(6) Tang, S.; Monot, J.; El-Hellani, A.; Michelet, B.; Guillot, R.; Bour, C.; Gandon, V. *Chem. Eur. J.* **2012**, *18*, 10239−10243.
(7) Han, X.; Li, H.; Hughes, R. P.; Wu, J. *Angew. Chem., Int. Ed.* **2012**, *51*, 10390−10393.
(8) Fricke, R.; Kosslick, H.; Lischke, G.; Richter, M. *Chem. Rev.* **2000**, *100*, 2303−2405.
(9) Pescarmona, P. P.; Janssen, K. P. F.; Jacobs, P. A. *Chem. Eur. J.* **2007**, *13*, 6562−6572.
(10) Stoica, G.; Santiago, M.; Jacobs, P. A.; Pérez-Ramírez, J.; Pescarmona, P. P. *Appl. Catal., A* **2009**, *371*, 43−53.
(11) Cates, C. D.; Myers, T. W.; Berben, L. A. *Inorg. Chem.* **2012**, *51*, 11891−11897.
(12) Myers, T. W.; Berben, L. A. *Inorg. Chem.* **2012**, *51*, 1480−1488.
(13) Carty, A. J.; Dymock, K. R.; Boorman, P. M. *Can. J. Chem.* **1970**, *48*, 3524−3529.
(14) Ivanov-Emin, B. N.; Nisel'son, L. A.; Rabovik, Y. I.; Larionova, L. E. *Russ. J. Inorg. Chem.* **1961**, *6*, 1142−1146.
(15) McPhail, A. T.; Miller, R. W.; Pitt, C. G.; Gupta, G.; Srivastava, S. C. *J. Chem. Soc., Dalton Trans.* **1976**, 1657−1661.
(16) Jiang, W.; Gorden, J. D.; Goldsmith, C. R. *Inorg. Chem.* **2012**, *51*, 2725−2727.
(17) Jiang, W.; Gorden, J. D.; Goldsmith, C. R. *Inorg. Chem.* **2013**, *52*, 5814−5823.
(18) Nam, W.; Valentine, J. S. *J. Am. Chem. Soc.* **1990**, *112*, 4977−4979.
(19) Rinaldi, R.; de Oliveira, H. F. N.; Schumann, H.; Schuchardt, U. *J. Mol. Catal. A* **2009**, *307*, 1−8.
(20) Kuznetsov, M. L.; Kozlov, Y. N.; Mandelli, D.; Pombeiro, A. J. L.; Shul'pin, G. B. *Inorg. Chem.* **2011**, *50*, 3996−4005.
(21) Phillips, B.; Starcher, P. S.; Ash, B. D. *J. Org. Chem.* **1959**, *23*, 1823−1826.
(22) Kamata, K.; Ishimoto, R.; Hirano, T.; Kuzuya, S.; Uehara, K.; Mizuno, N. *Inorg. Chem.* **2010**, *49*, 2471−2478.
(23) McGarrigle, E. M.; Gilheany, D. G. *Chem. Rev.* **2005**, *105*, 1563−1602.
(24) Quiñonero, D.; Morokuma, K.; Musaev, D. G.; Mas-Ballesté, R.; Que, L., Jr. *J. Am. Chem. Soc.* **2005**, *127*, 6548−6549.
(25) Shaik, S.; de Visser, S. P.; Ogliaro, F.; Schwarz, H.; Schröder, D. *Curr. Opin. Chem. Biol.* **2002**, *6*, 556−567.
(26) Urakawa, A.; Bürgi, T.; Skrabal, P.; Bangerter, F.; Baiker, A. *J. Phys. Chem. B* **2005**, *109*, 2212−2221.
(27) Frisch, M. J.; Trucks, G. W.; Schlegel, H. B.; Scuseria, G. E.; Robb, M. A.; Cheeseman, J. R.; Scalmani, G.; Barone, V.; Mennucci, B.; Petersson, G. A.; Nakatsuji, H.; Caricato, M.; Li, X.; Hratchian, H. P.; Izmaylov, A. F.; Bloino, J.; Zheng, G.; Sonnenberg, J. L.; Hada, M.; Ehara, M.; Toyota, K.; Fukuda, R.; Hasegawa, J.; Ishida, M.; Nakajima, T.; Honda, Y.; Kitao, O.; Nakai, H.; Vreven, T.; Montgomery, J. A.; Peralta, J. E.; Ogliaro, F.; Bearpark, M.; Heyd, J. J.; Brothers, E.; Kudin, K. N.; Staroverov, V. N.; Keith, T.; Kobayashi, R.; Normand, J.; Raghavachari, K.; Rendell, A.; Burant, J. C.; Iyengar, S. S.; Tomasi, J.; Cossi, M.; Rega, N.; Millam, J. M.; Klene, M.; Knox, J. E.; Cross, J. B.; Bakken, V.; Adamo, C.; Jaramillo, J.; Gomperts, R.; Stratmann, R. E.; Yazyev, O.; Austin, A. J.; Cammi, R.; Pomelli, C.; Ochterski, J. W.; Martin, R. L.; Morokuma, K.; Zakrzewski, V. G.; Voth, G. A.; Salvador, P.; Dannenberg, J. J.; Dapprich, S.; Daniels, A. D.; Farkas, O.; Foresman, J. B.; Ortiz, J. V.; Cioslowski, J.; Fox, D. J. *Gaussian 09*; Gaussian, Inc., Wallingford, CT, 2009.
(28) Zhao, Y.; Schultz, N. E.; Truhlar, D. G. *J. Chem. Theory Comput.* **2006**, *2*, 364−382.
(29) Raamat, E.; Kaupmees, K.; Ovsjannikov, G.; Trummal, A.; Kütt, A.; Saame, J.; Koppel, I.; Kaljurand, I.; Lipping, L.; Rodima, T.; Pihl, V.; Koppel, I. A.; Leito, I. *J. Phys. Org. Chem.* **2013**, *26*, 162−170.
(30) Marenich, A. V.; Cramer, C. J.; Truhlar, D. G. *J. Phys. Chem. B* **2009**, *113*, 6378−6396.
(31) Weinhold, F.LandisC. R. *Valency and Bonding: A Natural Bond Orbital Donor-Acceptor Perspective*; Cambridge University Press: Cambridge, U.K., 2005.
(32) Weinhold, F. *Discovering Chemistry with Natural Bond Orbitals*; Wiley: Hoboken, NJ, 2012.
(33) Glendening, E. D. *J. Phys. Chem. A* **2005**, *109*, 11936−11940.
(34) Glendening, E. D.; Badenhoop, J. K.; Reed, A. E.; Carpenter, J. E.; Bohmann, J. A.; Morales, C. M.; Weinhold, F. *NBO-5.9*; Theoretical Chemistry Institute, University of Wisconsin, Madison, WI, 2009.
(35) Cotton, F. A.; Wilkinson, G. *Advanced Inorganic Chemistry*, 5th ed.; Wiley: New York, 1988.
(36) Pearson, R. G. *J. Am. Chem. Soc.* **1963**, *85*, 3533−3539.
(37) Wiberg, K. B. *Angew. Chem., Int. Ed.* **1986**, *25*, 312−322.
(38) Novikov, A. S.; Kuznetsov, M. L.; Pombeiro, A. J. L.; Bokach, N. A.; Shul'pin, G. B. *ACS Catal.* **2013**, *3*, 1195−1208.
(39) Wang, Y.; Janardanan, D.; Usharani, D.; Han, K.; Que, L., Jr.; Shaik, S. *ACS Catal.* **2013**, *3*, 1334−1341.
(40) Zhang, X.; Furutachi, H.; Tojo, T.; Tsugawa, T.; Fujinami, S.; Sakurai, T.; Suzuki, M. *Chem. Lett.* **2011**, *40*, 515−517.
(41) Nakazawa, J.; Terada, S.; Yamada, M.; Hikichi, S. *J. Am. Chem. Soc.* **2013**, *135*, 6010−6013.